REMOTE MEASUREMENTS OF THERMAL TRANSMITTANCE WITHOUT APPROXIMATING A STEADY STATE

Jacob Estevam Schmiedt[1], Dhruvkumar Patel[1], Marc Röger[2], Philip Groesdonk[1], Bernhard Hoffschmidt[3]

[1] *Deutsches Zentrum für Luft- und Raumfahrt e.V. (German Aerospace Center), Institute of Solar Research, Karl-Heinz-Beckurts-Str. 13, 52428 Jülich, Germany, E-Mail: jacob.estevamschmiedt@dlr.de*

[2] *Deutsches Zentrum für Luft- und Raumfahrt e.V. (German Aerospace Center), Institute of Solar Research, Calle Doctor Carracido 44, 04005 Almería, Spain*

[3] *Deutsches Zentrum für Luft- und Raumfahrt e.V. (German Aerospace Center), Institute of Solar Research, Linder Höhe, 51147 Köln, Germany*

Abstract

The thermal transmittance of the building envelope is a key parameter that determines the energy performance of a building. In order to estimate the potential of refurbishment options, accurate information about the thermal transmittance is desirable. This information should be obtained with as little impact on the use of the building and in as little time as possible. The use of thermography for this purpose has the advantage that it allows for remote measurements without installation of sensors on the envelope. Additionally, a non-intrusive measurement method from outside of the buidling envelope is favorable. For that, a model calibration approach is proposed to increase the accuracy under varying environmental conditions and to reduce the measurement time for thermography from the outside. A simplified physical model with a small number of thermal resistor and capacitor elements is used to represent the building wall and simulate the heat flow under transient conditions. Its parameters are varied and chosen such that the best reproduction of the measured surface temperature is obtained. The uncertainty of the determined transmittance depends on the thermographic measurements and on the uncertainties in the boundary conditions which describe convective and radiative heat exchange and also have to be determined by measurements. The uncertainty analysis is performed using a Monte-Carlo sampling of all measured quantities.

Introduction

The thermal assessment of building envelopes is of strong interest because the high share of energy consumption in the building sector is a global concern. In most climate zones heating and cooling are responsible for the largest portion of energy consumption in the operation phase of a building. In the EU, private households alone were responsible for 27 % of the final energy consumption in 2020. More than 60 % of this energy is used for space heating and renewables contribute only about 27 % to this (European comission 2022).

A key indicator for the energy performance of a building envelope is the thermal transmittance (or U-value) that is given as the heat flux through an envelope element per temperature difference between inside and outside air. It has been observed frequently that design values or standard assumptions differ significantly from the thermal transmittance measured on real buildings (Gori et al. 2017, Teni et al. 2019, Li et al. 2014). In addition, for many old buildings the design values are not known. To close this so-called energy performance gap between simulation and real energy use (Wilde 2014, Dronkelaar et al. 2016) and to provide a solid basis for decisions about retrofit options, fast and accurate measurement methods measuring actual thermal transmittances of building envelopes are required. The thermal capacitance of building envelopes is another relevant quantity for its energy performance and the user comfort as it can flatten peaks in heating and cooling demand. For example, heat can be stored in the walls and floors, so that it can be released to the room when the outside temperature is extremely low for a short time (Olsthoorn 2017).

There are standardized methods to determine the thermal transmittances of building envelopes and their elements. These rely on averaging procedures to approximate steady-state conditions and, therefore, require relatively long measurement times of several days. The most common one is the heat flux meter (HFM) method (ISO 9869-1) which uses air temperature sensors and heat flux meters that are attached to a building element. Therefore, they only capture the heat flow through a small area and heterogeneities in rest of the envelop are not detected.

Thermography is a way to obtain data for extended areas and, therefore, detect heterogeneous structures, such as thermal bridges. Time series of thermographic images have also been used to determine the thermal transmittance of building envelope elements (ISO-9869-2 2018. Mahmoodzadeh, M. et al. 2022, Fokaides, P. A. et al. 2011, Marshall et al. 2018, Tejedor, B. et al. 2017). However, current methods either show large errors or are restricted to being used from inside of the building and require long measurement periods.

Model calibration is an approach that does not rely on the steady-state assumption and, therefore, is expected to give a higher accuracy while allowing shorter measurement times than the standardized methods (Gori et al. 2017). In order to capture also the dynamic behavior of the heat transport through the building, envelope models may contain also thermal capacitor or thermal mass (TM) elements. Thus, model calibration is also able to provide information about thermal capacitance. In literature, several approaches are found that use measured energy consumption and weather data to determine an overall heat transfer coefficient for the complete building envelope (Rouchier et al. 2018, Shamsi et al. 2020) which implies a strong influence of the user behavior on the results. Other approaches use heat flux meter data to identify the local thermal transmittance or thermal resistance at the respective measurement spot (Gori et al. 2017, Prada et al. 2019).

We have developed an approach that combines thermography and model calibration (Patel et al. 2023). It appears to be promising to be applied from the outside of a building while keeping measurement times short. In this paper, we recapiulate the method and an exemplary application in a setup with reduced environmental influences by wind and solar radiation. The core of the paper is a detailed evaluation of the uncertainty and reproducibility of the measurement results.

Methods

In order to determine the thermal resistance and transmittance, a simplified wall model will be calibrated which consists of two thermal mass elements and three thermal resistor elements. Thus, we have to solve a system of ordinary differential equations (ODEs). A sketch of the model is given in figure 1. The elements R1, R2 and R3 stand for thermal resistors. C1 and C2 stand for thermal capacitors. The elements air_temp_in, convection and rad_exchange on the bottom left represent the internal environmental conditions. The elements air_temp_out, rad_temp_out, convection and rad_exchange on the top right represent external environmental conditions. The prescribed temperatures on the inside and outside are determined by the data_input element.

A thermal resistor is charcterized by a resistance R and the heat flux through it is given by

$$q = \frac{1}{R_{\mathrm{therm}} A}(T_{\mathrm{l}} - T_{\mathrm{r}}),$$

where q is the heat flux, R_{therm} is the thermal resistance of the element, A its area, and T_{r} and T_{l} are the temperatures on the right and the left side of the resistor element respectively. The capacitor or TM elements stand are characterized by the thermal capacity C in the equation

$$C \frac{dT}{dt} = qA,$$

where C is the heat capacity and dT/dt is the derivative of its temperature T with respect to time. The connections with red lines in figure 1 mean that the temperatures at the connected points are set equal and that the heat flux into one element equals the heat flux out of the other element. If one element is connected to more than a single other element it means that the heat fluxes of those other elements are summed up.

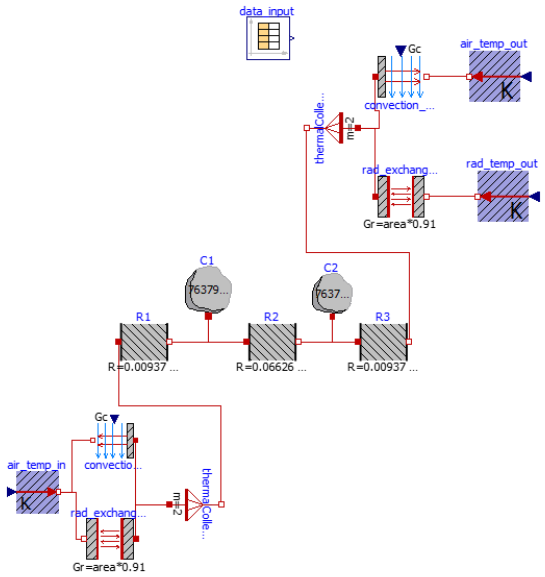

Figure 1: Graphical representation of the model with exemplary parameter values.

We consider convective and long-wave radiative heat exchange with the environment. So, on both sides of the wall, a convective term is added:

$$q_{\mathrm{conv}} = h_{\mathrm{in/out}}(T_{\mathrm{wall}} - T_{\mathrm{air}}),$$

where $h_{\mathrm{in/out}}$ is the convective heat transfer coefficient, T_{wall} is the surface temperature of the wall and T_{air} is the air temperature.

Based on the experimental setup described in section “Experiment”, we determine the convective heat transfer coefficient on the outside wall surface using the Nusselt number Nu (Ghajar 2015) as

$$h_{\text{out}} = \frac{Nu \cdot k}{L},$$

where k is the thermal conductivity of the wall and L is its height. For the convective heat transfer coefficient on the inside we use a literature value of h_{in} = 2.5 W/m^{2}K (ISO 6946:2017).

The long-wave radiation term is given by

$$q_{\text{lw}} = \varepsilon\sigma(T_{\text{wall}}^4 - T_{\text{surr}}^4),$$

where ε is the emissivity of the wall surface in the thermal infrared range between 7.5 and 14 µm, σ is the Stefan-Boltzmann constant and T_{surr} is a weighted average over the black body temperatures of the surrounding objects.

We end up with five unknown quantities R_1, R2, R3, C1, and C2. In our case, the wall has a symmetric structure, so that we can simplify

$$R_c \coloneqq R_2,$$

$$R_{\text{out}} \coloneqq R_1 = R_3,$$

$$C \coloneqq C_1 = C_2.$$

The resulting system of ODEs is solved numerically.

The thermal transmittance of the wall is given by

$$U = \frac{1}{h_{in}^{-1} + A(R_c + 2R_{out}) + h_{out}^{-1}}.$$

To determine the unknown quantities, we record a time series of surface temperatures using a series of thermographic images and the environmental conditions that determine the boundary conditions. Then we vary the unknown resistances and capacities of the model and minimize a target function χ^2 which is a function of the difference between the measured and the simulated surface temperatures. It is given by

$$\chi^2(\mathbf{R}, \mathbf{C}) = \sum_{i=1}^{N} \frac{1}{\sigma_i^2} \left(T_{\text{wall,meas}} - T_{\text{wall,model}}\right)^2,$$

where N is the number of time steps for that measurements were taken, i labels the individual time steps, and σ_i is the estimated uncertainty of the measured temperature at time step i. **R** is a vector that contains the resistance values of the model elements, and **C** is a vector that contains the capacities.

Uncertainty and Sensitivity

In order to study the reliability and reproducibility of the approach, we first compare the outcome of the calibration for different time intervals. In a second step, we perform an overall uncertainty analysis by a Monte-Carlo sampling. The uncertainties in the measured and estimated quantities are considered by drawing samples from a normal distribution with a standard deviation that is given by the measurement error. A list of these input quantities and the assumed standard deviations is given in table 2. Wherever quantities are taken from the literature, we motivate the standard deviation by comparing different literature values for the same quantity. The model calibration is then performed for each set of values, so that we obtain a distribution of results for the calibration outcome, e.g., the thermal resistance. In order to achieve an efficient sampling, we use the Latin Hypercube Sampling method.

We also study the sensitivity of the calibration results to changes in the individual input quantities. That is, the calibration is performed with a fixed offset in one of the measured or estimated input quantities.

For the uncertainty of the reference measurement, we follow the standard ISO 9868-1.

Experiment

In order to test the method, we heated up a small room which was enclosed by four walls and a roof. The whole structure was covered by a tent, so that no solar radiation could fall onto the walls and the wind speed on the inside and outside of the walls was close to zero. A thermal infrared (IR) microbolometer camera was placed on a tripod about 5 m from one of the walls. The wall was prepared for this experiment with reference temperature sensors (NTC sensors) on the inside and outside, heat flux meters on the inside and outside for reference measurements, and crumpled aluminium foil which serves as a diffuse reflector to measure the radiation temperature of the environment (Marshall et al. 2018). The air temperature close to the wall inside and outside of the room was also recorded. The radiation temperature of objects inside the room is assumed to be equal to the air temperature.

In front of the outside wall, we placed two self-made black bodies which were kept at different temperatures and served as references to correct for a drift of the temperature readings with the thermographic camera which appears due to changes in the housing temperature of the camera. The setup on the outside of the room can be seen in figure 2.

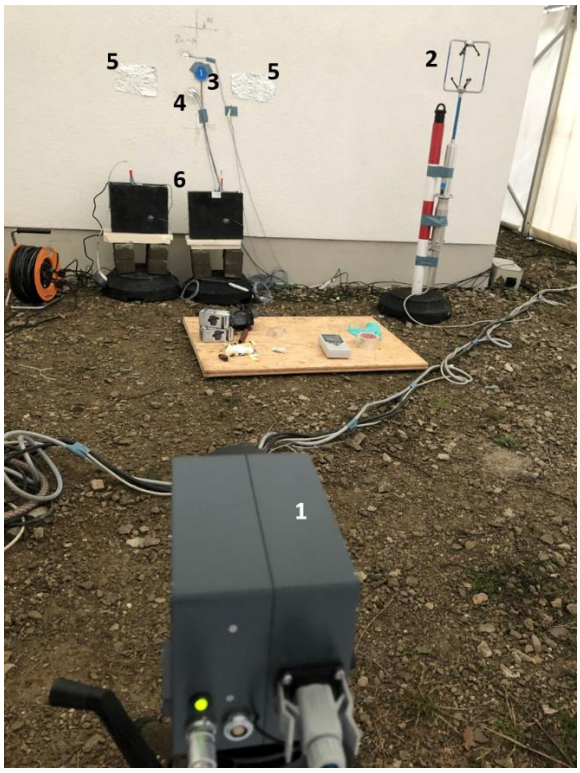

Figure 2: Measurement setup with infrared camera (1), an anemometer (2), a reference heat flux meter (3), reference surface temperature sensors (4) two reflectors made of aluminum foil (5), and two black bodies for reference temperature measurements (6).

Measurements were recorded for five consecutive days with one data point per minute. In parallel, the heat flux sensors on the inside of the wall were used to determine the thermal transmittance following the standard ISO 9869-1.

Results and Discussion

The recorded measurement data was evaluated and the calibration was performed for different time periods. We used the surface temperature average of a small area of a few cm^2 which was located in the center of one of the bricks below the plaster. In a preliminary test of the method with fixed **C** and variable **R**, we found that the calibration results are almost insensitive to **C**. This is consistent with the findings by Arregi et al. who argue that models with one or two TM are not well suited to determine the thermal capacity of a building element (Arregi et al. 2023). Therefore, we will focus on the results for the thermal resistance in the following and will not discuss our results for the thermal capacity.

Thermal Resistance

Table 1 shows the optimal values of $R = R_c + 2R_{out}$, the thermal transmittance U, the reference value of the transmittance R_{ref}, and the deviation between R and R_{ref} in percent which is denoted as d_R.

Table 1: Results of the calibration and transmittance calculation for various time intervals.

DAY	R [K/W]	U [W/m^{2}K]	R_{ref} [W/m^{2}K]	d_R [%]
1 – 5	0.085	1.47	0.064	33
1 – 3	0.083	1.51		30
2 – 4	0.086	1.46		34.4
3 – 5	0.087	1.44		36
1	0.081	1.55		26.6
2	0.085	1.47		32.8
3	0.086	1.46		34.4
4	0.088	1.41		37.5
5	0.087	1.44		35.9

The results of the calibration vary around the mean of R_{mean} = 0.085 K/W which is also the outcome for the longest time period. The standard deviation of the results is $\sigma_{days} = 0.002$. Both values are identical if they are calculated over all periods or only for the individual days. However, this is a relatively small sample size of measurements. Therefore, we determined the uncertainty of R also using the Monte-Carlo approach described above with the data for the complete five days. Table 2 shows the errors of the input quantities which were used as standard deviations of the distributions to draw samples.

Table 2: The errors of the input quantities for the model calibration. The second column shows the source of the input values.

QUANTITY	SOURCE	ERROR
Outside T_{air}	NTC sensor	$\pm$0.22 K
Outside T_{wall}	IR camera	$\pm$1.5 K
Outside T_{surr}	IR camera	$\pm$1.5 K
h_{out}	Nusselt number method	$\pm$0.5 W/m^{2}K
ε	Literature (Kolokotsa et al. 2012, Marshall et al. 1982, Engineering Toolbox 2003)	$\pm$0.3
Inside T_{air}	NTC sensor	$\pm$0.22 K
Inside T_{surr}	NTC sensor	$\pm$0.22 K
h_{in}	Literature (ISO 6946 2017)	$\pm$3.0 W/m^{2}K

As some combinations of input quantity values are unrealistic and do not allow for a good fit, we only use samples with a $\chi_r^2 \leq 0.1$. Figure 3 shows a histogram of the resulting distribution of thermal resistance outcomes.

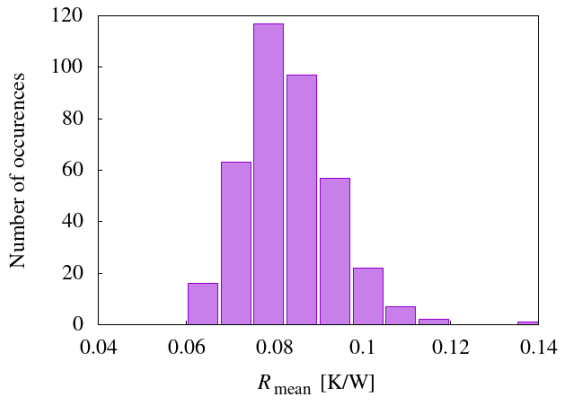

Figure 3: Histogram of occurrences for thermal resistance results in the Monte Carlo-based uncertainty analysis.

In order to check for convergence, we increased the sample size in steps. Figure 4 shows the mean R_{mean} and the standard deviation σ_R of the resulting distribution of thermal resistance. Both appear to be converged at a sample size of about 500. So, we obtain $R_{\text{mean}} = 0.083$ K/W and $\sigma_R = 0.011$ K/W which is significantly larger than σ_{days}. This means that the reference value is within the $2\sigma_R$ range of the thermal resistance from the model calibration.

The error of the reference measurement is determined according to the standard ISO 9869-1. The standard states that the error of a measurement lies between 14 % and 28 %. This means that in our case, the error is at least $\sigma_{\text{ref}} = 0.009$ K/W and may reach up to $\sigma_{\text{ref}} = 0.018$ K/W. So, the 1σ intervals of the reference measurement and the calibration approach likely overlap, indicating that the new approach of determining the thermal resistance from a model calibration using thermography data yields a result that is consistent with the reference method.

In order to distinguish the effect of the individual input quantities on the calibration result, we also did a sensitivity study where we varied the input quantities separately with a fixed positive and negative offset. The results are listed in table 3.

Table 3: The offset and the resulting deviation in the thermal resistance in the sensitivity analysis.

QUANTITY	OFFSET	THERMAL RESISTANCE (MIN, MAX)
Outside T_{air}	±0.5 K	(0.077, 0.089)
Outside T_{wall}	±1 K	(0.062, 0.116)
Outside T_{surr}	±1 K	(0.076, 0.090)
Inside T_{air}	±3 K	(0.080, 0.086)
h_{out}	±0.5 W/m²K	(0.079, 0.087)
h_{in}	±3 W/m²K	(0.082, 0.084)

Two offsets are chosen particularly large: the inside air temperature and the convective heat transfer coefficient on the inner side of the wall. These choices were made to account for the fact that a remote measurement ideally does not require any installation of sensors inside the building. In that case, these quantities would have to be estimated. Despite the large offset, the resulting difference in the thermal resistance is small at ±0.003 K/W. A similar difference of ±0.0035 K/W is caused by the comparatively small offset in the convective heat transfer coefficient on the outside. This means that a good model and accurate measurements of parameters that influence h_{out} are essential for the method. For a situation with full environmental conditions, i.e. without a tent, this implies that good wind speed measurement is an important requirement.

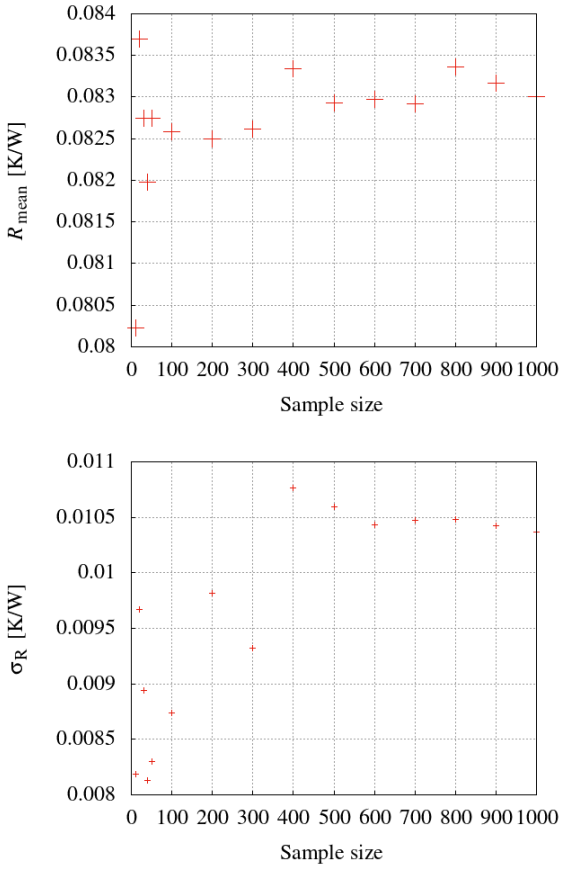

Figure 4: The outcome for R_{mean} and σ_R from Monte Carlo-sampling with increasing sample size.

The offset on T_{wall} and T_{surr} which are both measured with the infrared camera is smaller than the error that we considered before, but still lies in the range of common errors for modern microbolometer cameras. The large sensitivity of R with T_{wall} and T_{surr} that is found here stresses the importance of highly accurate temperature measurements with the camera and, in particular, of ways to detect and compensate possible drifts of the camera.

Conclusions

In this paper, we have summarized a new model calibration-based approach to determine the thermal transmittance of a wall by thermography. We have then presented an uncertainty and sensitivity analysis of the method.

We find that the calibration-based approach gives consistent results for different time periods. This indicates that at least under the controlled environmental conditions as in our experiment, a measurement time of a single day or less is likely to give a reliable result for the thermal transmittance.

The comparison with a reference measurement of the transmittance with a heat flux meter shows that the two measurements are compatible as their 1σ intervals overlap.

Finally, the variation of individual input quantities shows that an estimation of the indoor conditions without measuring them will likely have a very limited negative effect on the accuracy of the transmittance measurement by thermography and model calibration. Therefore, a fully remote measurement of the thermal transmittance without the need for installing sensors inside of the building appears possible. At the same time, variations in the convective heat transfer coefficient on the outside have a relatively strong impact on the results. This calls for a careful choice of the model for convective heat transfer and accurate wind measurements – in particular under full environmental conditions.

Literature

Arregi, B.; Garay-Martinez, R.; Carlos Ramos, J. 2023. Estimation of thermal resistance and capacitance of a concrete wall from in situ measurements: a comparison of steady-state and dynamic models, Energy and Buildings 296, p. 113393.

Dronkelaar, C.; Dowson, M.; Spataru, C.; Mumovic, D. 2016, Frontiers in Mechanical Engineering 1.

Engineering ToolBox, Emissivity Coefficients common Products [online] 2003, https://www.engineeringtoolbox.com/emissivity-coefficients-d_447.html.

European Commission. Statistical Office of the European Union 2022. Energy consumption in households, https://ec.europa.eu/eurostat/statistics-explained/index.php?title=Energy_consumption_in_households

Fokaides, P. A.; Kalogirou, S. A. 2011. Application of infrared thermography for the determination of the overall heat transfer coefficient (U-Value) in building envelopes, Applied Energy 88 (12), p 4358-4365.

Ghajar, A. J. 2015. Heat and mass transfer, McGraw-Hill.

Gori, V.; Marincioni, V.; Biddulph, P.; Elwell, C. A. 2017. Inferring the thermal resistance and effective thermal mass distribution of a wall from in situ measurements to characterise heat transfer at both the interior and exterior surfaces, Energy and Buildings 135, p 398-409.

ISO-6946 2017. Building components and building elements–thermal resistance and thermal transmittance–calculation method.

ISO-9869-1 2015. Thermal Insulation-Building Elements-In-situ Measurement of Thermal Resistance and Thermal Transmittance-Part 1: Heat Flow Meter Method.

ISO-9869-2 2018. Thermal Insulation-Building Elements-In-situ Measurement of Thermal Resistance and Thermal Transmittance - Part 2: Infrared method for frame structure dwelling.

Kolokotsa, D.; Maravelaki-Kalaitzaki, P.; Papantoniou, S.; Vangeloglou, E.; Saliari, M.; Karlessi, T.; Santamouris, M. 2012. Development and analysis of mineral based coatings for buildings and urban structures, Solar Energy 86 (5), p. 1648-1659.

Li, F. G. N.; Smith, A. Z. P.; Biddulph, P., Hamilton, I. G.; Lowe, R.; Mavrogianni, A.; Oikonomou, E.; Raslan, R.; Stamp, S.; Stone, A.; Summerfield, A. J.; Veitch, D.; Gori, V.; Oreszczyn, T. 2014. Solid-wall U-values: heat flux measurements compared with standard assumptions, Building Research & Information 43 (2), p 238-252.

Mahmoodzadeh, M.; Gretka, V.; Lee, I.; Mukhopadhyaya, P. 2022. Infrared thermography for quantitative thermal performance assessment of wood-framed building envelopes in Canada, Energy and Buildings 258, p 111807.

Marshall, A.; Francou, J.; Fitton, R.; Swan, W.; Owen, J.; Benjaber, M. 2018. Variations in the U-Value Measurement of a Whole Dwelling Using Infrared Thermography under Controlled Conditions, Buildings 8 (3).

Marshall, S. J.; Grot, R. A.; Wood, J. T. 1982. We Need To Know More About Infrared Emissivity, SPIE Proceedings, Thermal Infrared Sensing Applied to Energy Conservation in Building Envelopes.

Olsthoorn, D.; Haghighat, F.; Moreau, A.; lacroix, G. 2017. Building and Environment 118, p 113-127.

Patel, D.; Estevam Schmiedt, J.; Röger, M.; Hoffschmidt, B. 2023. A Model Calibration Approach to U-value Measurements with Thermography, Buildings 13 (9), p 2253.

Prada, A.; Gasparella, A.; Baggio, P. 2019. A Robust Approach For The Calibration Of the Material Properties in an Existing Wall, Proceedings of the 16th IBPSA Conference.

Rouchier, S.; Rabouille, M.; Oberlé, P. 2018. Calibration of simplified building energy models for parameter estimation and forecasting: Stochastic versus deterministic modelling, Building and Environment 134, p 181-190.

Shamsi, M.; Ali, U. Mangina, E. O'Donnell, J. 2020. A framework for uncertainty quantification in building heat demand simulations using reduced-order grey-box energy models, Applied Energy 275, p. 115141.

Tejedor, B.; Casals, M.; Gangolells, M.; Roca, X. 2017. Quantitative internal infrared thermography for determining in-situ thermal behaviour of façades, Energy and Buildings 151, p 187-197.

Teni, M.; Krstić, H.; Kosiński, P. 2019. Review and comparison of current experimental approaches for in-situ measurements of building walls thermal transmittance, Energy and Buildings 203, p 109417.

Wilde, P. 2014. Automation in Construction 41, p 40-49.